Available online at www.sciencedirect.com
ScienceDirect
Renewable and Sustainable Energy Reviews
11 (2007) 797–817

RENEWABLE
& SUSTAINABLE
ENERGY REVIEWS

www.elsevier.com/locate/rser

A critical review of convective heat transfer of nanofluids

Weerapun Daungthongsuk, Somchai Wongwises*

Fluid Mechanics, Thermal Engineering and Multiphase Flow Research Laboratory (FUTURE), Department of Mechanical Engineering, King Mongkut's University of Technology Thonburi, Bangmod, Bangkok 10140, Thailand

Received 3 May 2005; accepted 1 June 2005

Abstract

A nanofluid is a suspension of ultrafine particles in a conventional base fluid which tremendously enhances the heat transfer characteristics of the original fluid. Furthermore, nanofluids are expected to be ideally suited in practical applications as their use incurs little or no penalty in pressure drop because the nanoparticles are ultrafine, therefore, appearing to behave more like a single-phase fluid than a solid–liquid mixture. About a decade ago, several published articles focused on measuring and determining the effective thermal conductivity of nanofluids, some also evaluated the effective viscosity. There are only a few published articles on deriving the forced convective heat transfer of nanofluids. The purpose of this article is to summarize the published subjects respect to the forced convective heat transfer of the nanofluids both of experimental and numerical investigation.

Keywords: Nanofluids; Ultrafine; Effective thermal conductivity; Effective viscosity; Forced convective heat transfer

Contents

*Corresponding author. Tel.: +66 2 470 9115; fax: +66 2 470 9111.
E-mail address: somchai.won@kmutt.ac.th (S. Wongwises).

1364-0321/$ - see front matter
doi:10.1016/j.rser.2005.06.005

1. Introduction

Improvements to make heat transfer equipment more energy efficient would need to focus on miniaturization on the one hand and an astronomical increase in heat flux on the other. Heat transfer fluids such as water, mineral oil and ethylene glycol play a vital role in many industrial processes, including power generation, chemical processes, heating or cooling processes, and microelectronics. The poor heat transfer properties of these common fluids compared to most solids is a primary obstacle to the high compactness and effectiveness of heat exchangers. The essential initiative is to seek the solid particles having thermal conductivities several hundreds of times higher than those of conventional fluids. An innovative idea is to suspend ultrafine solid particles in the fluid for improving the thermal conductivity of a fluid. Many types of particle, such as metallic, non-metallic and polymeric, can be added into fluids to form slurries. However, the usual slurries, with suspended particles in the order of millimeters or even micrometers may cause some severe problems. The abrasive action of the particles causes the clogging of flow channels, erosion of pipelines and their momentum transfers into an increase in pressure drop in practical applications. Furthermore, they often suffer from instability and rheological problems. In particular, the particles tend to settle rapidly. Thus, although the slurries give better thermal conductivities, they are not practical.

The use of particles of nanometer dimension was first continuously studied by a research group at the Argonne National Laboratory around a decade ago. Choi [1] was probably the first one who called the fluids with particles of nanometer dimensions 'nano-fluids'. Compared with suspended particles of millimeter-or-micrometer dimensions, nanofluids show better stability and rheological properties, dramatically higher thermal conductivities, and no penalty in pressure drop. Several published literature have mainly focused on the prediction and measurement techniques in order to evaluate the thermal conductivity of nanofluid. Recently, Trisaksri and Wongwises [2] reviewed the literature on the general heat transfer characteristics of nanofluids. It was found that only a few papers have discussed on the convective heat transfer of nanofluids. The purpose of this article is to review the literature mentioning convective heat transfer of nanofluids, including the experimental and theoretical investigations.

2. Experimental approach

A several years ago, the nanofluid has been found to be an attractive heat transport fluids. It has exhibited a significant potential for heat transfer augmentation relative to the conventional pure fluids. It has been expected to be suitable for the engineering application without severe problems in pipeline and with little or no penalty in pressure drop. However, the earlier researches revealed that most studies of the transport properties of the nanofluid were focused on the thermal conductivity. The convective heat transfer of nanofluids has received comparatively little attention in literature. There are few publications dealing with the convective heat transfer of nanofluids. The most productive studies have been continuously carried out by the following researchers.

Nomenclature

A	cross section area, m^2
C	concentration of liquid solution, kg_w/kg_{sol}
C_p	specific heat, J/kg K
d	nanoparitcle diameter, m
D	inner diameter of the tube, m
g	acceleration of gravity, m/s^2
h	heat transfer coefficient, W/m^2 K
H	humidity ratio of the air, kg_w/kg_a
k	thermal conductivity of the nanofluid, W/m K
L	length of the test tube, m
$\dot{m}$	mass flow rate, kg/s
Nu	Nusselt number
ΔP	pressure drop, Pa
Pe	Peclet number
Pr	Prandtl number
q	heat flux, W/m^2
Q	heat transfer rate, W
r	radius of tube, m
R	radius of disc, m
Re	Reynolds number
S	perimeter, m
t	thickness, m or time in the Lattice Boltzmann method
T	temperature, °C
u	mean velocity, m/s
U	overall heat transfer coefficient, W/m^2 K
v	velocity in y-direction, m/s
V	volume, m^3
w	velocity in z-direction, m/s
x	distance along the tube, m or x-coordinate
y	y-coordinate
z	z-coordinate
α	thermal diffusivity, m^2/s
β	thermal dispersion coefficient, N/m^2 K
ε	rate of dissipation (for k–ε turbulent model)
λ	friction factor
ω	tangential coordinate, rad
ϕ	volume fraction
Φ	inclination angle, degree
ψ	thermal diffusivity coefficient
Ψ	mass diffusivity, m^2/s
κ	turbulent kinetic energy (for k–ε turbulent model)
ρ	density, kg/m^3
τ	tensor of the dispersed thermal conductivity
υ	viscosity, m^2/s

Subscript

a	annulus or air
d	particle
des	desiccant
D	dispersion effect
f	fluid
hf	heating fluid
i	inside
in	inlet
lm	log mean
m	mean
o	out
out	outlet
nf	nanofluid
r	radial direction
T	turbulent
w	tube wall
x	axial direction

Li and Xuan [3], and Xuan and Li [4] presented an experimental system to investigate the convective heat transfer coefficient and friction factor of nanofluids for laminar and turbulent flow in a tube. The sample nanofluid used in this study was deionized water with a dispersion of Cu particles with below 100 nm diameter. The nanofluids, with different particle volume percentages, were used to determine the effect of the nanoparticle concentration on the heat transfer coefficient, the percentages being 0.3, 0.5, 0.8, 1, 1.5 and 2%. The Reynolds number of the nanofluids varied within the range of 800–25,000. The experimental apparatus was mainly composed of a reservoir tank, a pump, a pipeline, a test section, a cooler, and a fluid collection tank. Test section was a straight brass tube with 10 mm inner diameter and 800 mm length and a 3.5 kW electric heater was used to obtain a constant wall heat flux boundary condition. To prevent the aggregation of the nanoparticles in the base fluid, a fatty acid was used as a dispersant to cover the nanoparticles. The experimental apparatus of their work was depicted in Fig. 1.

The heat transfer coefficient of the nanofluids is calculated from the following equations

$$Nu_{\mathrm{nf}} = \frac{h_{\mathrm{nf}} D}{k_{\mathrm{nf}}} \tag{1}$$

$$h_{\mathrm{nf}} = \frac{q}{T_{\mathrm{w}} - T_{\mathrm{f}}} \tag{2}$$

The experimental results illustrated that the convective heat transfer coefficient of the nanofluids varied with the flow velocity and volume fraction as well as being higher than the base fluid at the same conditions. Compared with water, the Nusselt number of the nanofluid with 2% volume fraction of Cu particles was 60% higher. Furthermore, the Dittus-Boelter equation was not valid for the prediction of the Nusselt number of the nanofluids at various volume fractions. From the experimental data, new heat transfer

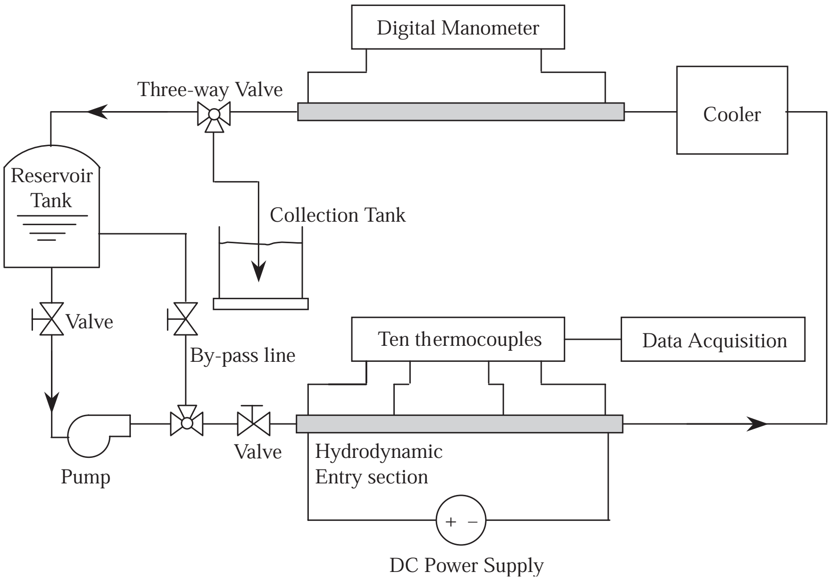


Fig. 1. The experimental apparatus of Xuan and Li [3] and, Li and Xuan [4].

correlations for the prediction of the heat transfer coefficient of nanofluids flowing in a tube could be established in the following form:

For laminar flow

$$Nu_{\mathrm{nf}} = 0.4328\left(1.0 + 11.285\phi^{0.754} Pe_{\mathrm{d}}^{0.218}\right)\mathrm{Re}_{\mathrm{nf}}^{0.333} Pr_{\mathrm{nf}}^{0.4} \tag{3}$$

For turbulent flow

$$Nu_{\mathrm{nf}} = 0.0059\left(1.0 + 7.6286\phi^{0.6886} Pe_{\mathrm{d}}^{0.001}\right)\mathrm{Re}_{\mathrm{nf}}^{0.9238} Pr_{\mathrm{nf}}^{0.4} \tag{4}$$

where Nu is the Nusselt number, Pe is the Peclet number, Re is the Reynolds number, and Pr is the Prandtl number.

$$Pe_{\mathrm{d}} = \frac{u_{\mathrm{m}} d_{\mathrm{p}}}{\alpha_{\mathrm{nf}}} \tag{5}$$

$$\mathrm{Re}_{\mathrm{nf}} = \frac{u_{\mathrm{m}} D}{\upsilon_{\mathrm{nf}}} \tag{6}$$

and

$$Pr_{\mathrm{nf}} = \frac{\upsilon_{\mathrm{nf}}}{\alpha_{\mathrm{nf}}} \tag{7}$$

In order to calculate these parameters, the thermal diffusivity of the nanofluid was defined as

$$\alpha_{\mathrm{nf}} = \frac{k_{\mathrm{nf}}}{\left(\rho C_p\right)_{\mathrm{nf}}} = \frac{k_{\mathrm{nf}}}{(1-\phi)\left(\rho C_{\mathrm{p}}\right)_{\mathrm{f}} + \phi\left(\rho C_{\mathrm{p}}\right)_{\mathrm{d}}} \tag{8}$$

In the case of the pressure drop, the results indicate that the friction factor of the nanofluid was almost equal to those of water under the same flow velocity and did not vary

with the volume fraction. This implies that the nanofluids cause no penalty to pump power and the single-phase friction factor correlation can be used for more accurate predictions. The friction factor of the nanofluids was determined from the following equation:

$$\lambda_{\mathrm{nf}} = \frac{\Delta P_{\mathrm{nf}} D}{L} \frac{2g}{u_{\mathrm{m}}^2} \tag{9}$$

Yang et al. [5] reported experimental results which illustrated the convective heat transfer coefficient of graphite nanoparticles dispersed in liquid for laminar flow in a horizontal tube heat exchanger. Nanoparticles of different sources were used in this study and focused on an aspect ratio (l/d) of about 0.02 (like a disc), because the addition of large aspect ratio particles into a fluid may dramatically increase viscosity compared with the single-phase. In this study, two series of nanofluids with different base fluids were used. The experiments were performed within the following ranges: the volume flow rates were between 62–507 cm^3/min, the Reynolds number varied between 5–110, and the heating fluid temperature between 50–70 °C. This article intended to study the effects of the Reynolds number, volume fraction, temperature, nanoparticle source, and type of base fluid on the convective heat transfer coefficient. The experimental system used in this study was shown schematically in Fig. 2.

The following calculation procedure was used to evaluate the heat transfer coefficient of the nanofluids.

The heat transfer rate into the nanofluids is

$$Q_{\mathrm{nf}} = \dot{m} Cp (T_{\mathrm{out}} - T_{\mathrm{in}}) \tag{10}$$

The heat transfer from the heating fluids is

$$Q_{\mathrm{hf}} = \dot{m}_{\mathrm{hf}} Cp_{\mathrm{hf}} (T_{\mathrm{out}} - T_{\mathrm{in}})_{\mathrm{hf}} \tag{11}$$

The energy balance between the heating fluid and the process fluid were differences around 25%. This is common for a small-scale testing equipment.

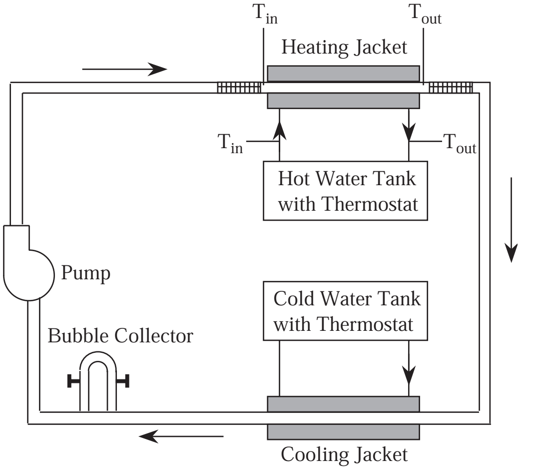


Fig. 2. Schematic diagram of the experimental apparatus of Yang et al. [5].

The overall heat transfer resistance relationship is used to determine the heat transfer coefficient of the nanofluids, h_{nf}:

$$\frac{1}{U} = \frac{1}{h_{\mathrm{nf}}\left(A_i/A_o\right)} + \frac{D_{\mathrm{o}}}{2k}\ln\frac{D_{\mathrm{o}}}{D_{\mathrm{i}}} + \frac{1}{h_{\mathrm{o}}} \tag{12}$$

The overall heat transfer coefficient can then be determined from

$$U = \frac{Q}{A_{\mathrm{o}}\Delta T_{\mathrm{lm}}} \tag{13}$$

The Monrad and Pelton's equation for turbulent flow in annuli was used to calculate the outside heat transfer coefficient, h_{o}, as follows:

$$Nu = 0.020\mathrm{Re}^{0.8}\mathrm{Pr}^{1/3}\left(D_2/D_1\right)^{0.53} \tag{14}$$

Subscript 2 and 1 mean the outer and inner diameter of the annulus, respectively. The equivalent diameter, D_{e}, was used instead of the typical diameter, D.

$$D_{\mathrm{e}} = \frac{D_{\mathrm{i,a}}^2 - D_{\mathrm{o}}^2}{D_{\mathrm{o}}} \tag{15}$$

The experimental results illustrated that the heat transfer coefficient increased with the Reynolds number and the particle volume fraction. For example, at 2 wt% the heat transfer coefficient of the nanofluids was moderately increased compared with the base fluid, but at 2.5 wt% it was 22% higher than the base fluid at 50 °C fluid temperature and 15% higher at 70 °C. Several factors may lead to smaller improvements in heat transfer enhancement of nanofluids with increased fluid temperature. One is the rapid alignment of nanoparticles in less viscous fluids, leading to less contact between the nanoparticles. A second factor is that depletion of particles in the near-wall fluid phase could lead to a lower thermal conductivity layer near the wall. Two graphite nanoparticle sources at same particle loading give different heat transfer coefficient, as in the case of different base fluids. This may have been caused by particle shape, morphology or surface treatment. This means that one type of nanoparticle is more effective than another in augmenting the heat transfer coefficient of the nanofluid. Moreover, the correlation established by Li and Xuan [4] for laminar flow of nanofluids gave a higher heat transfer coefficient than that calculated from the experimental data. This may be because the effect of particle aspect ratio was not included. Similarly, the single-phase correlation of laminar flow in tubes failed to predict the convective heat transfer coefficient of nanofluids.

All of the experimental data were used to develop a new heat transfer correlation for the prediction the heat transfer coefficient of laminar flow nanofluids in a more convenient form by modifying the Seider-Tate equation [6] as follow:

$$\Omega = Nu_{\mathrm{nf}}Pr_{\mathrm{nf}}^{-1/3}\left(\frac{L}{D}\right)^{1/3}\left(\frac{\mu_{\mathrm{f}}}{\mu_{\mathrm{w}}}\right)^{-0.14} = a\mathrm{Re}_{\mathrm{nf}}^{b} \tag{16}$$

where a and b are the various constants which depend on the experimental conditions.

Wen and Ding [7] presented an experimental study which evaluated the convective heat transfer coefficient of γAl_2O_3 nanoparticles suspended in deionized water for laminar flow in a copper tube, focusing in particular on the entrance region. The various concentrations of nanoparticles (0.6, 1.0, and 1.6%) were tested under a constant wall heat flux. The experimental apparatus mainly consisted of a straight copper tube with 970 mm length,

4.5 ± 0.02 mm inner diameter, and 6.4 ± 0.05 mm outer diameter as a test section. A 300 W silicon rubber flexible heater was used to keep a constant heat flux boundary condition. A peristaltic pump was used to deliver a maximum flow rate of 10 l/min. The flow rate was controlled by adjusting rotational speed of the pump. In order to stabilize the nanoparticles, sodium dodecylbenzene sulfonate (SDBS) was used as a dispersant. Their experimental apparatus was shown schematically in Fig. 3.

The heat transfer coefficient and the Nusselt number of the nanofluids were calculated from the following equations:

$$Nu_{\mathrm{nf,x}} = \frac{h_{\mathrm{nf,x}} D}{k_{\mathrm{nf}}} \tag{17}$$

$$h_{\mathrm{nf,x}} = \frac{q}{T_{\mathrm{w,x}} - T_{\mathrm{f,x}}} \tag{18}$$

The energy balance was used to determine the fluid temperature profile along the test tube as follows:

$$T_{\mathrm{f,x}} = T_{\mathrm{in}} + \frac{qSx}{\rho C_{\mathrm{p}} u A} \tag{19}$$

The results showed that the local heat transfer coefficient varied with the Reynolds number and volume fraction. In particular, the entrance region illustrated that the use of nanofluids affected a pronounced increase in the heat transfer coefficient causing a decrease in the thermal boundary layer thickness and will decrease along the tube length.

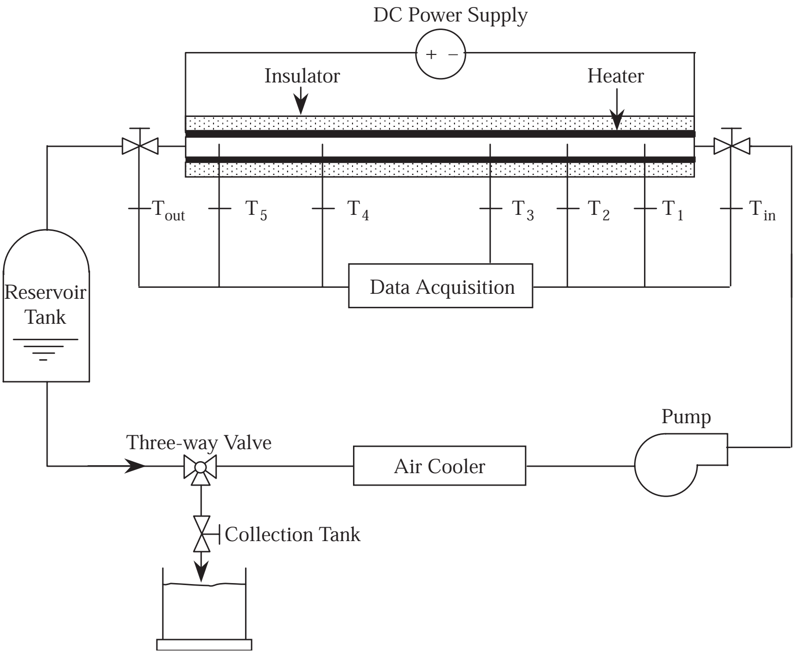


Fig. 3. Schematic diagram of the experimental apparatus of Wen and Ding [7].

This behavior implied that it might be possible to create a 'smart entrance' region to meet the highest performance of nanofluids. Furthermore, the Shah correlation for laminar flow and the Dittus-Boelter equation for turbulent flow do not coincide with the Nusselt number between the experimental results and the calculated values.

3. Mathematical approach

Similar to the experimental investigation, many researchers devoted to formulate the appropriate correlations for prediction of the thermal conductivity of the nanofluid. It is difficult to establish any formulated theory for the prediction of the accurate heat transfer behavior of the nanofluid because the several complex phenomena may coexist in the main flow e.g. sedimentation, Brownian force, dispersion, and friction force between the fluid and the solid particles. Some researchers treat the nanofluid more like a fluid rather than a liquid–solid mixture. There are few articles taking the nanofluid into account as the multi-phase feature. Some detailed reviews mentioned above are shown as follows:

Xuan and Li [8] presented a method for preparing some nanofluid samples and introduced a theoretical study of thermal conductivity. They used the transient hot-wire method for measurements. They then suggested a dispersion model or single-phase model to describe the heat transfer performance of nanofluids flowing in a tube. The nanoparticles used in this article were Cu particles with 100 nm diameter, respectively, suspended in water and mineral oil. Oleic acid and laurate salt were used as dispersants in order to stabilize the particles in the mineral oil and water, respectively. For Cu–mineral oil, the results showed that the suspension reached a stabilized state within about 1 week and had no sedimentation with a fill of 22 wt%. In the case of Cu–water nanofluid suspension with 9 wt% laurate salt, vibrated by a ultrasonic vibrator, the results indicated that the nanoparticles can suspend more 30 h than in stationary state. This behavior implied that the fluid viscosity might be an important factor affecting the dispersion and stability of the particles. Moreover, this study illustrated that the Hamilton and Crosser model [9] and Wasp model [10] for predicting thermal conductivity can be applied to obtain an approximate solution in the absence of a sophisticated formula. Using the transient hotwire method to measure the thermal conductivity, the results showed that the thermal conductivity remarkably varied with the volume fraction of the particles. There are two different approaches to analyze the heat transfer enhancement. One is the two-phase model and other is the single-phase model. Although the first model describes an understanding of the functions of both liquid phase and solid phase in the heat transfer process, it needs a long time for computation and a high performance computer. The second model, assuming that both the liquid and particle phases are in thermal equilibrium and flow at the same velocity, is simpler and needs less computation time. The purpose of their work aimed to develop a modified single-phase model to describe the heat transfer process of nanofluids flowing in tubes. The governing equations were expressed as follow:

$$\frac{\partial T}{\partial t}+u\frac{\partial T}{\partial x}=\left(\phi+\frac{\beta_{\mathrm{x}}}{(\rho C_{\mathrm{P}})_{\mathrm{nf}}}\right)\frac{\partial^2 T}{\partial x^2}+\frac{1}{r}\frac{\partial}{\partial r}\left[\left(\phi+\frac{\beta_r}{(\rho C_{\mathrm{P}})_{\mathrm{nf}}}\right)r\frac{\partial T}{\partial r}\right] \tag{20}$$

If the axial temperature distribution is ignored, Eq. (20) can be reduced as

$$\frac{\partial T}{\partial t}+u\frac{\partial T}{\partial x}=\frac{1}{r}\frac{\partial}{\partial r}\left[\left(\phi+\frac{\beta_{\mathrm{r}}}{(\rho C_{\mathrm{P}})_{\mathrm{nf}}}\right)r\frac{\partial T}{\partial r}\right] \tag{21}$$

The boundary conditions for this situation are as follows:

$$T|_{r=R} = T_{\rm w} \text{ and } T|_{x=0} = T_{\rm o} \tag{22}$$

The application of the separation of variables method for plug flow, the following solution was obtained:

$$\frac{T - T_{\rm w}}{T_{\rm o} - T_{\rm w}} = 2\sum_{m=1}^{\infty} {\rm e}^{-\theta_m^2 \bar{x}/\bar{P}e} \frac{J_0(\theta_m \bar{r})}{J_1(\theta_m)\theta_m} \tag{23}$$

where $\bar{r} = r/R$, $\bar{x} = x/L$, $Nu = 2{\rm Rh}/k^*_{\rm nf}$, $Pe^* = uL/\phi^*$, $\bar{P}e = Pe^*\left(R/L\right)^2$ and eigenvalues $\theta_{\rm m}$'s are the positive roots of the following equation:

$$J_0(\theta_m) = 0 \tag{24}$$

The heat balance can be expresses as

$$-k^*_{\rm nf}\frac{\partial T}{\partial r}\bigg|_{r=R} = h(T_{\rm b} - T_{\rm w}) \tag{25}$$

The analytical correlation of the Nusselt number is then given by

$$Nu = \frac{\sum_{m=1}^{\infty} {\rm e}^{-\theta_m^2 \bar{x}/\bar{P}e}}{\sum_{m=1}^{\infty} {\rm e}^{-\theta_m^2 \bar{x}/\bar{P}e}/\theta_m^2} \tag{26}$$

For presence of the dispersion in axial and radial direction, Eq. (20) and the modified Dankwerts's boundary conditions (Eqs. (27a) and (27b)) in the axial direction and the boundary condition in radial direction Eq. (22) give solution (Eq. (28)).

$$-k^*_{\rm nf}\frac{\partial T}{\partial x} = uA\rho C_{\rm P}(T_0 - T) \text{ at } x = 0, \tag{27a}$$

$$\frac{\partial T}{\partial x} = 0 \text{ at } x = L \tag{27b}$$

$$\frac{T - T_{\rm w}}{T_{\rm o} - T_{\rm w}} = 2\sum_{m=1}^{\infty} \frac{X(\bar{x})}{\left[X(0) - X'(0)/Pe^*\right]} \frac{J_0(\theta_m \bar{r})}{J_1(\theta_m)\theta_m} \tag{28}$$

where $X(\bar{x})$ and $X'(\bar{x})$ are defined as follows:

$$X(\bar{x}) = m_2 {\rm e}^{m_2 + m_1 \bar{x}} - m_1 {\rm e}^{m_1 + m_2 \bar{x}}$$

$$X'(\bar{x}) = m_1 m_2 \left({\rm e}^{m_2 + m_1 \bar{x}} - {\rm e}^{m_1 + m_2 \bar{x}}\right)$$

$$m_{1,2} = \frac{Pe^* \pm \sqrt{Pe^{*2} + 4\theta_m^2 \left(L/R\right)^2}}{2}$$

The eigenvalues are described in Eq. (24). Thus, the Nusselt number correlation for the nanofluids is obtained from

$$Nu = \frac{\sum_{m=1}^{\infty} X(\bar{x})/\left[X(0) - X'(0)/Pe^*\right]}{\sum_{m=1}^{\infty} \left[X(\bar{x})/\left[X(0) - X'(0)/Pe^*\right]\right]/\theta_m^2} \tag{29}$$

It should be noted that Eqs. (26) and (29) are derived for constant wall temperature and need the iteration procedure to solve the problem. The Nusselt number for the other boundary conditions can derive with the same method.

Finally, this study expressed that either theoretical expressions or experimental work needed to explain the heat transfer process of nanofluids, in which several phenomena may coexist in the main flow.

Xuan and Roetzel [11] presented two different approaches to determine some fundamentals to predict the convective heat transfer coefficient of nanofluids under the assumption that they behaved like a single-phase liquid rather than a normal solid–liquid mixture. They included both the effects of transport properties and thermal dispersion of the nanofluid. The first model treated the nanofluid as a single-phase fluid and the second model as a multi-phase and dispersed fluid. In a conventional approach, the assumptions were no slip velocity between the particles and liquid phase and that they were in a thermal equilibrium state. The nanofluid behaved like a common pure liquid. This implied that the whole equation of continuity, motion and energy for a single-phase fluid had been applied directly to the nanofluid. Similar to the Xuan and Li model [8], the Hamilton and Crosser model [9] and Wasp model [10] for predicting the thermal conductivity of nanofluid give rough estimations. For a modified conventional approach, called the dispersion model, the slip velocity between the solid–liquid mixture may not be zero causing many factors, such as Brownian force, gravity, friction force between the solid–liquid mixture, Brownian diffusion, sedimentation, and dispersion to happen simultaneously in the main flow. The details of two approaches are expressed as follows:

For the conventional approach, the general form of the energy equation for the incompressible pure fluid with negligible viscous dissipation is

$$\frac{\partial T}{\partial t} + \nabla \cdot uT = \nabla \cdot (\alpha_{\mathrm{f}} \nabla T) \tag{30}$$

This equation is suitable to explain the heat transfer process of the nanofluid. This means that the heat transfer equation for the single-phase fluids can extend to the nanofluid directly. It should be noted that the thermal properties used in this equation are those of nanofluids. For this reason, the dimensionless heat transfer correlations of the single-phase fluid can be applicable for the nanofluid, so

$$Nu = 3.66 \text{ (For fully developed laminar flow in tube, } T_{\mathrm{w}} = \text{const.)} \tag{31a}$$

$$Nu = 0.023\mathrm{Re}^{0.8}\mathrm{Pr}^{1/3} \text{ (For turbulent flow in tube)} \tag{31b}$$

For the modified conventional approach, the irregular movement of the ultrafine particles led to little disturbances of both the temperature, T', and velocity of the nanofluid, u'. Hence, the real temperature and velocity averages are expressed as

$$T = \langle T \rangle^f + T' \tag{32a}$$

$$\boldsymbol{u} = \langle \boldsymbol{u} \rangle^f + \boldsymbol{u}' \tag{32b}$$

where $\langle T \rangle^f = (1/V_{\mathrm{f}}) \int_{V_{\mathrm{f}}} T \mathrm{d}V$, $\langle \boldsymbol{u} \rangle^f = (1/V_{\mathrm{f}}) \int_{V_{\mathrm{f}}} \boldsymbol{u} \mathrm{d}V$ and $(1/V_{\mathrm{f}}) \int_{V_{\mathrm{f}}} T' \mathrm{d}V = 0$

By the procedure demonstrated by Kaviany [12] and assuming that the boundary surface between the fluid and the particles is so small, Eq. (30) can be rewritten as

$$(\rho C_{\mathrm{p}})_{\mathrm{nf}}\left[\frac{\partial\langle T\rangle'}{\partial t}+\langle \boldsymbol{u}\rangle^{f}\nabla\cdot\langle T\rangle^{f}\right]=\nabla\cdot\left(k_{\mathrm{nf}}\nabla\langle T\rangle^{f}\right)-(\rho C_{\mathrm{p}})_{\mathrm{nf}}\nabla\langle \boldsymbol{u}'T'\rangle^{f} \tag{33}$$

The chaotic movement of the ultrafine particles in the flow gives the thermal dispersion (the second term on the right hand side of Eq. (33)). Therefore, the heat flux resulted from the dispersion in the nanofluid flow can be expressed as:

$$q_{\mathrm{D}}=(\rho C_{\mathrm{P}})_{\mathrm{nf}}\langle \boldsymbol{u}'T'\rangle^{f}=-\tau_{\mathrm{D}}\cdot\nabla\langle T\rangle^{f} \tag{34}$$

where τ is the tensor of the dispersed thermal conductivity. Thus, Eq. (33) can be rewritten as

$$\left[\frac{\partial\langle T\rangle'}{\partial t}+\langle u\rangle^{f}\nabla\cdot\langle T\rangle^{f}\right]=\nabla\cdot\left[\left(\alpha_{\mathrm{nf}}\mathrm{I}+\frac{\tau_{\mathrm{D}}}{(\rho C_{\mathrm{P}})_{\mathrm{nf}}}\right)\cdot\nabla\langle T'\rangle^{f}\right] \tag{35}$$

Then, the energy balance equation for the nanofluid can be given as

$$(\rho C_{\mathrm{P}})_{\mathrm{nf}}\frac{\partial\langle T\rangle'}{\partial t}+(\rho C_{\mathrm{P}})_{\mathrm{nf}}\langle u\rangle\cdot\nabla\langle T\rangle=(\rho C_{\mathrm{P}})_{\mathrm{nf}}\nabla(\psi\cdot\nabla\langle T\rangle) \tag{36}$$

where ψ may be called the total effective thermal diffusivity tensor. It combines the molecular effect and the thermal dispersion effect. ψ is defined as follows:

$$\psi=\frac{k_{\mathrm{nf}}I}{(\rho C_{\mathrm{P}})_{\mathrm{nf}}}+(1-\phi)\psi_{\mathrm{D}} \tag{37}$$

It is anticipated that the thermal dispersion tensor is a function of the flow pattern, properties of the base fluid and the nanoparticles, dimensions and shape of the nanoparticles, and volume fraction of the nanoparticles.

The energy equation for the nanofluid flowing inside a tube for this situation may be expressed as

$$\frac{\partial T}{\partial t}+u\frac{\partial T}{\partial x}=\frac{1}{r}\frac{\partial}{\partial r}\left[\left(\alpha_{\mathrm{nf}}+\frac{k_{\mathrm{D,r}}}{(\rho C\mathrm{p})_{\mathrm{nf}}}\right)r\frac{\partial T}{\partial r}\right] \tag{38}$$

For taking the thermal dispersion in the axial direction into account, so

$$\frac{\partial T}{\partial t}+u\frac{\partial T}{\partial x}=\frac{1}{r}\frac{\partial}{\partial r}\left[\left(\alpha_{\mathrm{nf}}+\frac{k_{\mathrm{D,r}}}{(\rho C\mathrm{p})_{\mathrm{nf}}}\right)r\frac{\partial T}{\partial r}\right]+\frac{\partial}{\partial x}\left[\left(\alpha_{\mathrm{nf}}+\frac{k_{\mathrm{D},x}}{(\rho C\mathrm{p})_{\mathrm{nf}}}\right)\frac{\partial T}{\partial x}\right] \tag{39}$$

The thermal diffusivity coefficients can be found from the derivation of Taylor [13] and Aris [14]. Unfortunately, there is no theoretical and experimental work established on the dispersed thermal diffusivity of the nanofluid. The k_{D} appearing in Eqs. (38) and (39) can be calculated by Plumb [15] and Hunt and Tien [16].

To take the effect of thermal dispersion into account, the surface heat flux can be expressed as

$$q=-\left(k_{\mathrm{nf}}\frac{\partial T}{\partial r}+k_{\mathrm{D},r}\frac{\partial T}{\partial r}\right)|_{r=R} \tag{40}$$

Similar to the procedure proposed by Nield and Bejan [17], the dimensional analysis of the above equation formally resulted in the heat transfer correlation of the nanofluid as

follows:

$$Nu_x = [1 + C^* Pef'(0)]\theta'(0)\mathrm{Re}^m \quad (41a)$$

with considering the flow pattern, Eq. (41a) can be modified to Eq. (41b)

$$Nu_x = [1 + C^* Pe^n f'(0)]\theta'(0)\mathrm{Re}^m \quad (41b)$$

In which $Pe = (ru_{\mathrm{m}}/\alpha_{\mathrm{nf}})$, C^* is an unknown constant determined from experiment, m and n depend on the flow pattern, f is dimensionless velocity, θ is dimensionless temperature, and f' and θ' are the derivatives of the dimensionless velocity and dimensionless temperature, respectively.

Maiga et al. [18] presented a mathematical formulation and numerical method to determine the forced convective heat transfer and wall shear stress for the laminar and turbulent regions of water–γAl_2O_3 and ethylene glycol–γAl_2O_3 flowing inside a uniformly heated tube. The solid–liquid mixture takes a single-phase behavior into account, so the slip velocity between the phases was neglected. Furthermore, the local thermal equilibrium of the mixture and symmetry in flow were considered. For the turbulent flow region, the Reynolds-averaged Navier-Stokes equation and κ–ε turbulent model were used to describe the stresses and heat flux of the nanofluids. The conditions of the numerical simulations were as follow: the heated tube had 0.01 m diameter and 1.0 m length. In the situation of laminar flow, the Reynolds number was fixed at 250 and the constant heat flux was varied between 10–250 W/m^2. For turbulent flow, the constant heat flux was fixed at 500,000 W/m^2 and the Reynolds number was varied in the range of 10,000–50,000. The problem configuration for this study is shown in Fig. 4.

Under the above conditions the governing equations depicted in a (R, ω and Z) coordinate system are as follows:

$$\nabla \cdot (\rho u) = 0 \quad (42)$$

$$\nabla \cdot (\rho u u_i) = -\partial P/\partial X_i + \nabla \cdot (\mu \nabla u_i) + S_i \quad (43)$$

$$\nabla \cdot (\rho u C_{\mathrm{P}} T) = \nabla \cdot (k \nabla T) \quad (44)$$

where $u = (u_{\mathrm{R}}, u_\omega, u_Z)$ is the velocity vector, X_i represents a spatial direction ($X_i = R$, ω and Z), and S_i represents the remaining viscous term corresponding to the coordinate system.

− for the radial direction, $R\,(i = 1)$;

$$S_1 = \frac{\rho u_\varpi u_\varpi}{R} - \mu\left[\frac{u_R}{R^2} + \frac{2}{R^2}\frac{\partial u_\varpi}{\partial \varpi}\right] \quad (45)$$

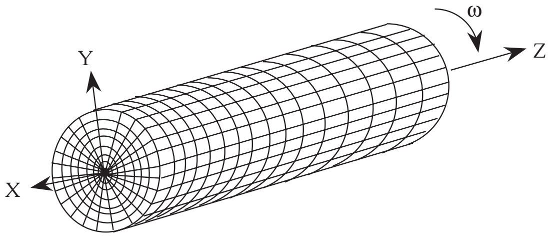


Fig. 4. The problem configuration in the study of Maiga et al. [18].

– for the tangential direction, $\omega\,(i=2)$;

$$S_2 = \mu\left[\frac{2}{R^2}\frac{\partial u_R}{\partial \varpi} - \frac{u_\varpi}{R^2}\right] - \frac{\rho u_R u_\varpi}{R} \tag{46}$$

– for the axial direction, $Z\,(i=3)$;

$$S_3 = 0 \tag{47}$$

For the turbulent flow regime, this article shows the application of the famous semi-empirical κ–ε turbulent model. The equations for this case are described as follow:

$$\nabla\cdot(\rho\boldsymbol{u}\kappa) = \nabla\cdot\left[\mu + \frac{\mu_T}{Pr_{T,\kappa}}\nabla\kappa\right] + G_\kappa - \rho\varepsilon \tag{48}$$

$$\nabla\cdot(\rho\boldsymbol{u}\varepsilon) = \nabla\cdot\left[\mu + \frac{\mu_T}{Pr_{T,\varepsilon}}\nabla\varepsilon\right] + C_{1\varepsilon}(\varepsilon/\kappa)G_\kappa + C_{2\varepsilon}\rho\varepsilon^2/\kappa \tag{49}$$

where G_κ is the generation of turbulence kinetic energy due to the mean velocity gradients, and μ_{T} is the turbulent viscosity calculated from

$$\mu_T = \rho C_\mu \kappa^2/\varepsilon \tag{50}$$

Various constants in the above equations are as follows:

$$C_{1\varepsilon} = 1.44;\;\; C_{2\varepsilon} = 1.92;\;\; C_\mu = 0.09;\;\; Pr_{T,\kappa} = 1.0;\;\; \text{and}\;\; Pr_{T,\varepsilon} = 1.3 \tag{51}$$

The numerical results illustrated that the heat transfer and the wall friction of nanofluids increased with increasing the particle concentration and the ethylene glycol–γAl_2O_3 gave higher heat transfer enhancement than the water–γAl_2O_3. Then, the heat transfer performance of the nanofluids was more pronounced with the increase of the Reynolds number for the turbulent flow region.

Roy et al. [19] proposed a numerical investigation to evaluate the heat transfer and wall shear stress for radial laminar flow in a cooling system of water–γAl_2O_3 nanofluids compared with water, glycol, and oil as base fluids. All assumptions used in this study were similar to Maiga et al. [18] who took the nanofluid as an incompressible fluid. The geometric configuration of this work is shown in Fig. 5.

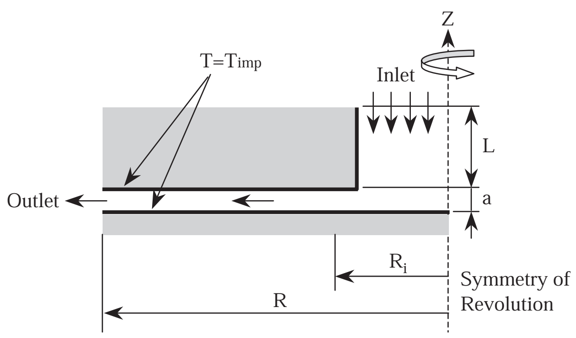


Fig. 5. The geometric configuration in the study of Roy et al. [19].

The governing equations in the cylindrical coordinate (R, Z) and symmetry systems can be given as follows:

$$\nabla \cdot (\rho u) = 0 \tag{52}$$

$$\nabla \cdot (\rho u u_i) = -\nabla P + \nabla \cdot (\mu \nabla u_i) + S_i, \quad i = 1, 2 \tag{53}$$

$$\nabla \cdot (\rho u C_P T) = \nabla \cdot (k \nabla T) \tag{54}$$

− for the radial direction, $R(i = 1)$;

$$S_1 = -\mu \left[\frac{u_R}{R^2} \right] \tag{55}$$

− for the axial direction, $Z(i = 1)$;

$$S_2 = 0 \tag{56}$$

The results show that the heat transfer rate and wall shear stress were higher with increasing particle concentration and Reynolds number.

Nguyen et al. [20] introduced a numerical simulation to determine the efficiency of water–γAl_2O_3 and ethylene glycol–γAl_2O_3 nanofluids for the cooling of a high-heat output microprocessor under laminar forced flow inside a heat sink. The simulation set-up consisted of a $50 \times 50 \times 10$ mm rectangular slot with a 3×48 mm fluid flow cross-section. Assumptions used in this article were laminar flow, uniform velocity and temperature profile at the inlet section. The contact area for heat exchange was 10×10 mm. The problem configuration for this study was sketched in Fig. 6.

The numerical results indicate that the average heat transfer coefficient of nanofluids varied higher with the volume fraction and Reynolds number and the ethylene glycol–γAl_2O_3 nanofluid gave higher heat transfer coefficient than the water–γAl_2O_3 nanofluid.

Ali et al. [21] reported the mathematical and numerical formulation to determine heat and mass transfer between air and falling solution film in a cross-flow heat exchanger for the dehumidification and cooling process. The Cu nanoparticles were added into the solution in order to evaluate their effect in the augmentation of the heat and mass transfer process. Two models, proposed by Xuan and Roetzel [11], were used in this study. Furthermore, the assumptions of this article were as follow: (1) laminar and steady state flow; (2) thermal properties of the air and the solution are constant except for the thermal

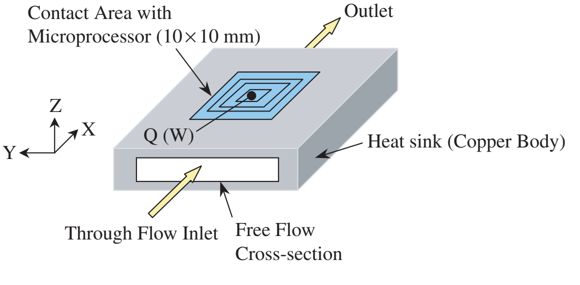


Fig. 6. The problem configuration in the study of Nguyen et al. [20].

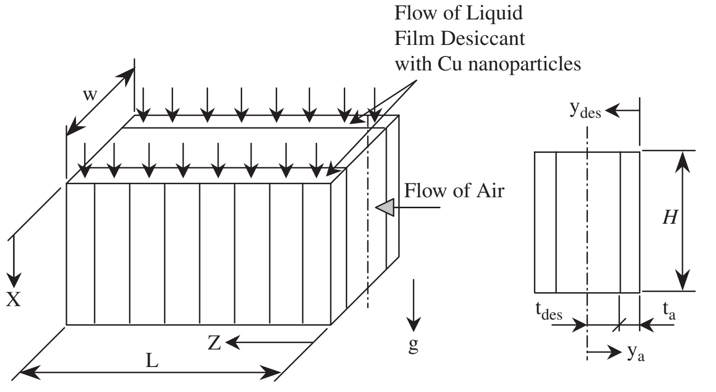


Fig. 7. Schematic diagram of problem configuration of Ali et al. [21].

conductivity of the solution; (3) gravitational force of the air is neglected; (4) constant film thickness and (5) fully developed velocity profile for fluids. The schematic diagram of this work was shown in Fig. 7.

The governing conservation equations of mass, momentum, energy, and mass diffusion are illustrated in two portions; air and solution (liquid film) as follows:

- For the air

$$\frac{\partial w_z}{\partial Z} = 0 \tag{57}$$

$$\frac{\partial P_a}{\partial Z} = \mu_a \left(\frac{\partial^2 w_a}{\partial y_a^2} \right) \tag{58}$$

$$\rho_a Cp_a w_a \frac{\partial T_a}{\partial z} = k_a \frac{\partial^2 T_a}{\partial y_a^2} \tag{59}$$

$$w_a \frac{\partial H_a}{\partial z} = \Psi_a \frac{\partial^2 C_a}{\partial y_a^2} \tag{60}$$

- For the solution (liquid film)

$$\frac{\partial u_{des}}{\partial x} = 0 \tag{61}$$

$$\rho_{des} g + \mu_{des} \left(\frac{\partial^2 u_{des}}{\partial y_{des}^2} \right) = 0 \tag{62}$$

$$(\rho Cpu)_{des} \frac{\partial T_{des}}{\partial x} = \frac{\partial}{\partial y_{des}} \left[(k_{nf} + k_{dis}) \frac{\partial T_{des}}{\partial y_{des}} \right] \tag{63}$$

$$u_{des} \frac{\partial C_{des}}{\partial x} = \Psi_{des} \frac{\partial^2 C_{des}}{\partial y_{des}^2} \tag{64}$$

The energy balance equation at interface between air and film desiccant is

$$k_a \frac{\partial T_a}{\partial y_a} + \rho_a \Psi_a h_{fg} \frac{\partial H_a}{\partial y_a} = -k_{des} \frac{\partial T_{des}}{\partial y_{des}} \tag{65}$$

at $y_a = t_a$, $y_{des} = t_{des}$, $0 \le x \le H$ and $0 \le z \le L$

The mass balance at the interface is

$$\rho_a \Psi_a \frac{\partial H_a}{\partial y_a} = -(\rho\Psi)_{des} \frac{\partial C_{des}}{\partial y_{des}} \tag{66}$$

at $y_a = t_a$, $y_{des} = t_{des}$, $0 \le x \le H$ and $0 \le z \le L$

With the suitable boundary conditions, the velocities for both air and film desiccant are obtained analytically from Eqs. (58) and (62) as follows:

$$w_a(y_a) = \frac{1}{2\mu_a} \frac{\partial P_a}{\partial z} (y_a^2 - t_a^2) \tag{67}$$

$$u_{des}(y_{des}) = \frac{\rho_{des} g}{\mu_{des}} y_{des} \left(t_{des} - \frac{y_{des}}{2} \right) \tag{68}$$

The air side pressure drop and the solution thickness are calculated from

$$\frac{\partial P_a}{\partial z} = -\frac{3}{2} \frac{\mu_a \dot{m}_a}{H \rho_a t_a^3} \tag{69}$$

$$t_{des} = \left[\frac{3 \dot{m}_{des} u_{des}}{\rho_{des} g} \right]^{1/3} \tag{70}$$

The results illustrated that the dehumidification and cooling process increased with the following parameters: low air Reynolds number, high Cu particle volume fraction, increases in the height and length of the channel, and decreases in the channel width. Also, it was found that an increase in Cu volume fraction led to more stability of the solution.

Ali and Vafai [22] presented the mathematical and numerical formulations to evaluate the effects of the inclination angel of parallel-and-counter-flow on heat and mass transfer between air and falling desiccant film, with Cu nanoparticles suspended. As Ali et al. [21], the same assumptions were held and two approach models, introduced by Xuan and Roetzel [11] where used in this literature. Then, the simulated conditions used in this study are summarized as follow: low and high air Reynolds number for the inclined parallel flow arrangement, and low and high air Reynolds number for the inclined counter flow configuration. The problem configuration for this study was shown schematically in Fig. 8.

Similar to Ali et al. [21], the general governing equations (continuity, momentum, energy, and mass diffusion for air and the desiccant film) for both parallel flow and counter flow can be given by

- For the air

$$\frac{\partial u_a}{\partial x_1} + \frac{\partial v_a}{\partial y_1} = 0 \tag{71}$$

$$\rho_a \left(u_a \frac{\partial u_a}{\partial x_1} + v_a \frac{\partial u_a}{\partial y_1} \right) = -\frac{\partial P}{\partial x} + \mu_a \left(\frac{\partial^2 u_a}{\partial y_1^2} \right) \tag{72}$$

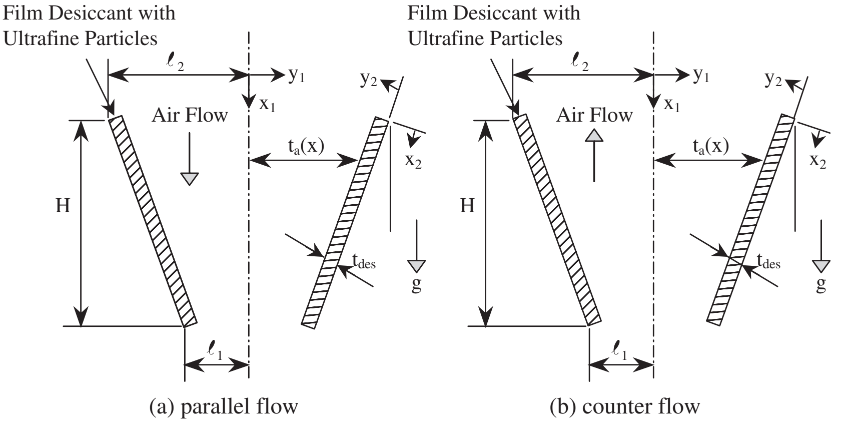


Fig. 8. The geometric configurations in the study of Ali and Vafai [22].

$$\rho_a\left(u_a\frac{\partial v_a}{\partial x_1}+v_a\frac{\partial v_a}{\partial y_1}\right)=-\frac{\partial P}{\partial x}+\mu_a\left(\frac{\partial^2 v_a}{\partial y_1^2}\right) \tag{73}$$

$$\rho_a C_P\left(u_a\frac{\partial T_a}{\partial x_1}+v_a\frac{\partial T_a}{\partial y_1}\right)=K_a\left(\frac{\partial^2 T_a}{\partial y_1^2}\right) \tag{74}$$

$$u_a\frac{\partial H}{\partial x_1}+v_a\frac{\partial H}{\partial y_1}=\Psi_a\left(\frac{\partial^2 H}{\partial y_1^2}\right) \tag{75}$$

− For the desiccant film

$$\frac{\partial u_{des}}{\partial x_2}=0 \tag{76}$$

$$\rho_{des}g+\mu_{des}\left(\frac{\partial^2 u_{des}}{\partial y_2^2}\right)=0 \tag{77}$$

$$(\rho C_P u)_{des}\frac{\partial T_{des}}{\partial x_2}=\frac{\partial}{\partial y_2}\left[(k_{nf}+k_{dis})\frac{\partial T_{des}}{\partial y_2}\right] \tag{78}$$

$$u_{des}\frac{\partial C}{\partial x_2}=\Psi_{des}\frac{\partial^2 C}{\partial y_2^2} \tag{79}$$

In order to solve the governing equations of the air, the coordinate transformations are needed for both inclined parallel and counter flow. The simulation conditions used in this work are in the range of low and high air Reynolds number.

From the numerical results it could be concluded that the dehumidification and cooling process of air and regeneration process of the liquid desiccant are enhanced with increasing inclination angle for both parallel-and-counter flow-channels. Moreover, the effective thermal conductivity of the liquid desiccant varied with the Cu nanoparticles and

the thermal dispersion and low desiccant concentration led to enhancement of the dehumidification process.

Xuan et al. [23] proposed the thermal Lattice Boltzmann model to display the flow features and heat transfer process of Cu–water nanofluid flowing inside a channel. The important advantage of this method was that it took the molecular dynamics into account and bridged the gap of microscopic or macroscopic phenomena of the nanofluids. For application of this method to model the thermal fluid flow problem, there are two existing methods: the multispeed (MS) and the double-distribution-function (DDF), the latter method being used in this article. This led to two separate distribution functions as follow: the temperature is treated as a passive diffusing scalar, and it is simulated by a distribution function independent of density distribution, respectively. The feature point of the Lattice Boltzmann method is the assumption that the particles are mesoscopically located at a series of lattices and their distributions correspond to the Boltzmann distribution. For simulation of heat transfer characteristics of the nanofluid, the viscosity dissipation term in the Lattice Boltzmann equation for energy transport will be neglected. The equation is given by

$$T_i(x + e_i\Delta t, t + \Delta t) - T_i(x, t) = -\frac{\lfloor T_i(x,t) - T_{\mathrm{i}}^{\mathrm{eq}}(x,t)\rfloor}{\tau_T}; \quad i = 1,2,3,4 \tag{80}$$

where e_{i} is the lattice velocity vector, τ_{T} is the collision-relaxation time constant for the temperature distribution. $T_{\mathrm{i}}^{\mathrm{eq}}$ is the equilibrium function for the temperature which is defined as

$$T_{\mathrm{i}}^{\mathrm{eq}} = A_i T + B_i \frac{(e_i \cdot \mathrm{Tu})}{\mathrm{c}^2}; \quad i = 1,2,3,4 \tag{81}$$

where c is the reference lattice velocity $(\Delta x/\Delta t)$

By using the Lattice Boltzmann method to model the nanofluid, the dynamic factors influencing the flow behavior of the nanofluid must be considered first. Without external forces, the nanoparticles are under influence of the buoyancy force, gravitational force, Brownian force, drag force and dispersion force resulting from the repulsive potential [13]. Hence, the sum of the total forces vector acting on the nanoparticle per unit lattice volume (V) is given by

$$F = n(F_{\mathrm{A}} + F_{\mathrm{B}} + F_{\mathrm{D}} + F_{\mathrm{H}})/V \tag{82}$$

where n is the number of the nanoparticles in a given lattice, F_{A} is the dispersion force, F_{B} is the Brownian force, F_{D} is the drag force, and F_{H} represents the buoyancy and gravitational force, respectively. These several variables are defined as

$$F_{\mathrm{A}} = \sum_{i=1}^{8} n_i \frac{\partial V_{\mathrm{A}}}{\partial r_i} \tag{83}$$

$$V_{\mathrm{A}} = -\frac{1}{6}A\left(\frac{2a^2}{L^2 - 4a^2} + \frac{2a^2}{L^2} + \mathrm{In}\frac{L^2 - 4a^2}{L^2}\right) \tag{84}$$

$$F_{\mathrm{B}} = G_i\sqrt{C/\Delta t} \tag{85}$$

$$C = 2\lambda k_{\mathrm{B}} T; \qquad \lambda = 6\pi\eta a \tag{86}$$

$$F_{\mathrm{D}} = -6\pi\mu a\Delta u \tag{87}$$

$$F_{\mathrm{H}} = -\frac{4}{3}\pi a^3 g\Delta\rho \tag{88}$$

where a is the radius of the nanoparticle, $\Delta\rho$ and Δu are the density and the velocity difference between the nanoparticle and the base fluid, respectively, λ is the friction coefficient, k_{B} is the Boltzmann constant, G_{i} is the zero mean (unit variance independent Gaussian random number), L is the distance between center-to-center of the particles, and A represents Hamaker constant which accounts for the material properties but not for the configuration shape.

The numerical results showed that, for 1% volume fraction the Nusselt number of Cu–water nanofluid was 27% higher than that of pure water at the same Reynolds number. Moreover, fluctuations of the Nusselt number of the nanofluid taking place along the main flow direction may cause random motion of the particles suspended in the fluid.

4. Conclusion

Evidently, nanofluids have great potential for heat transfer enhancement and are highly suited to application in practical heat transfer processes. This offers an opportunity for engineers to develop highly compact and effective heat transfer equipment. Several published articles show that the heat transfer coefficient of nanofluids are much higher than the common-base fluid and give little or no penalty in pressure drop. The main reasons for the heat transfer enhancement of the nanofluids may roughly be listed as follow: the suspended nanoparticles increase the thermal conductivity of the fluids, and the chaotic movement of ultrafine particles increases fluctuation and turbulence of the fluids which accelerates the energy exchange process. Furthermore, that the numerous correlations for single-phase fluid have clearly failed to predict the heat transfer coefficients of nanofluids may be caused by the complicated phenomena that coexist in the main flow. However, some sophisticated correlations for predicting the heat transfer performance of nanofluids have been established. At the present time, the uses of the nanofluids ar still remaining in early stages of development. Therefore, urgent theoretical and experimental research works is needed in order to clearly understand and accurately predict their hydrodynamic and thermal characteristics. Generally, many researchers indicated that nanofluids behave like pure fluids because the suspended particles are ultrafine. However, at present, no formulated advanced theory exists to explain the behaviour of nanofluids by considering them is as multi-component materials.

Acknowledgements

The authors would like to express their appreciation to the Thailand Research Fund (TRF) for providing financial support in this study.

References

[1] Choi US. Enhancing Thermal Conductivity of Fluids with Nanoparticles. ASME FED 1995;231:99–103.

[2] Trisaksri V, Wongwises S. Critical Review of Heat Transfer Characteristics of the Nanofluids, Renewable and Sustainable Energy Reviews, 2005 (in press).

[3] Xuan Y, Li Q. Investigation on Convective Heat Transfer and Flow Features of Nanofluids. ASME J Heat Transfer 2003;125:151–5.

[4] Li Q, Xuan Y. Convective Heat Transfer and Flow Characteristics of Cu-Water Nanofluid. Science in China (Series E) 2002;45(4):408–16.

[5] Yang Y, Zhang ZG, Grulke EA, Anderson WB, Wu G. Heat Transfer Properties of Nanoparticle-in-Fluid Dispersions (Nanofluids) in Laminar Flow. Int J Heat Mass Transfer 2005;48(6):1107–16.

[6] Sieder EN, Tate GE. Heat Transfer and Pressure Drop of Liquids in Tube. Ind. Eng. Chem. 1936;28(12): 1429–35.

[7] Wen D, Ding Y. Experimental Investigation into Convective Heat Transfer of Nanofluids at the Entrance Region under Laminar Flow Conditions. Int J Heat Mass Transfer 2004;47:5181–8.

[8] Xuan Y, Li Q. Heat Transfer Enhancement of Nanofluids. Int J Heat Fluid Flow 2000;21:58–64.

[9] Hamilton RL, Crosser OK. Thermal Conductivity of Heterogeneous Two-Component System. I&EC Fundamentals1 1962:182–91.

[10] Wasp FJ. Solid-Liquid Flow Slurry Pipeline Transportation. Berlin: Trans. Tech. Pub.; 1977.

[11] Xuan Y, Roetzel W. Conceptions for Heat Transfer Correlation of Nanofluids. Int J Heat Mass Transfer 2000;43:3701–7.

[12] Kaviany M. Principles of Heat Transfer in Porous Media. Berlin: Springer; 1995.

[13] Taylor GI. The Dispersion of Matter in Turbulent Flow in a Pipe. Proc. Roy. Soc. (London) A223, 1954: 446–68.

[14] Aris R. On the Dispersion of a Solute in a Fluid Flowing Through a Tube. Proc. Roy. Soc. (London) A235 1956:67–77.

[15] Plumb OA. The Effect of Thermal Dispersion on Heat Transfer in Packed Bed Boundary Layer. Proc. ASME JSME Thermal Engineering Joint Conference2 1983:17–22.

[16] Hunt ML, Tien CL. Effects of Thermal Dispersion on Forced Convection in Fibrous Media. Int. J. Heat and Mass Transfer 1988;31:301–9.

[17] Nield DA, Bejan A. Convection in Porous Media, 2nd ed. Berlin: Springer; 1998.

[18] Maiga SEB, Nguyen CT, Galanis N, Roy G. Heat Transfer Behaviours of Nanofluids in a uniformly Heated Tube. Superlattices and Microstructures 2004;35:543–57.

[19] Roy G, Nguyen CT, Lajoie PR. Numerical Investigation of Laminar Flow and Heat Transfer in a Radial Flow Cooling System with the Use of Nanofluids. Superlattices and Microstructures 2004;35:497–511.

[20] Nguyen CT, Roy G, Maiga SEB, Lajoie PR., 2004, Heat Transfer Enhancement by Using Nanofluids for Cooling of High Output Microprocessor, www.electronics-cooling.com/html/2004_nov_techbrief.html.

[21] Ali A, Vafai K, Khaled ARA. Analysis of Heat and Mass Transfer between Air and Falling Film in a Cross Flow Configuration. Int J Heat Mass Transfer 2004;47:743–55.

[22] Ali A, Vafai K. An Investigation of Heat and Mass Transfer between Air and Desiccant Film in an Inclined Parallel and Counter Flow Channels. Int. J Heat Mass Transfer 2004;47:1745–60.

[23] Xuan Y, Yu K, Li Q. Investigation on Flow and Heat Transfer of Nanofluids by the Thermal Lattice Boltzmann Model, Progress in. Computational Fluid Dynamics 2005;5(1/2):13–9.